46th Annual Review of Progress
in Quantitative Nondestructive Evaluation
QNDE2019
July 14-19, 2019, Portland, OR, USA

QNDE2019-1234

PASSIVE GUIDED WAVE TOMOGRAPHY FOR PIPES INSPECTION

Tom Druet[1], Huu Tinh Hoang, Bastien Chapuis
CEA LIST
Gif-sur-Yvette, France

Emmanuel Moulin
Université Polytechnique Hauts de France
Valenciennes, France

ABSTRACT

Structural Health Monitoring (SHM) consists in embedding sensors in a structure like aircraft fuselages, pipes or ship hulls in order to detect defects (for example cracks or corrosion in metallic materials or delamination in composite materials) before a serious damage occurs in the structure. Guided elastic waves emitted by a sensor and propagating to another one are often used as the physical way of detecting the defect. However, the implementation of SHM systems is restricted in many situations by the necessity to store or to harvest the electric energy necessary to emit the waves and also by the intrusiveness of the sensors. Guided wave tomography imaging is able to localize and quantify the severity of the defect when it comes to loss of thickness such as corrosion or erosion. However, it needs many sensors (generally piezoelectric –PZT– transducers) and it has a cost, particularly in terms of intrusiveness. Passive guided wave tomography, which uses ambient ultrasonic waves that are naturally present in the structure, is a promising method to design an SHM system with minimal power consumption and intrusiveness since no energy is required to emit the waves. In this paper the application of passive tomography to pipe inspection and comparison with classical "active" guided waves tomography approach are described.

Keywords: passive methods, guided wave tomography, SHM

1. INTRODUCTION

The maintenance has a prominent role from both cost point of view and security. The Structural Health Monitoring (SHM) consists in acquiring and analyzing data from sensors embedded in a structure in order to evaluate its health [1]. A physical way to interrogate large and thin structures such as aircraft fuselages, pipes or ship hulls can be offered by guided elastic waves emitted and received by a network of piezoelectric transducers (PZTs). Guided wave tomography algorithms are able to not only localize but also quantify the severity of defects consisting in a loss of thickness such as corrosion or erosion. However, it needs many sensors (generally piezoelectric –PZT– transducers) and it has a cost, particularly in terms of intrusiveness.

An interesting possibility is to design a guided wave based SHM system with low intrusiveness thanks to the use of guided wave tomography with undersampled data. Indeed, less sensors are used compared to the optimal number but it is still possible to obtain a satisfactory image of the defect. Another interesting possibility which also answers to the electric energy consumption issue is to work only with receivers of elastic waves. To achieve this, passive methods based on elastic noise measurements can be used to retrieve the response between the sensors without using active (piezoelectric) sources [2] [3]. We present here studies of passive guided wave tomography of pipes.

2. MATERIALS AND METHODS

In this section is presented the passive guided wave tomography. First the basis of the passive method used here is given and then the main steps of guided wave tomography are recalled.

2.1 Passive method

Guided wave tomography is commonly applied to active data: each sensor acts successively as a source whereas other sensors measure the propagated signals. In this work, the imaging is obtained from passive data, that is, the signal corresponding to each emitter-receiver couple is reconstructed thanks to the cross-correlation of the ambient noise measured simultaneously by every couple of sensors [4].

In the following, the ambient noise φ is a space-time stationary random field that is also delta correlated in space and time. Let's consider a plate as a 2D domain and two sensors placed at points x and y. Let us denote V_x, respectively V_y, the ambient noise acquired by the sensor at x, respectively y, on the time interval $[0, T]$, $T > 0$. The cross-correlation C_T of these two signals is

[1] Contact author: tom.druet@cea.fr

$$C_T(t,x,y) = \frac{1}{T}\int_0^T V_x(\tau)V_y(t+\tau)\,\mathrm{d}\tau. \quad (1)$$

One can then show [4] that

$$\frac{\mathrm{d}\,C_T}{\mathrm{d}t} \propto H_{xy}(t) - H_{xy}(-t), \quad (2)$$

where H_{xy} is the impulse response of the system formed by the plate and the sensors, the sensor at x acting as a source while the one at y acts as a receiver. Note that if the domain is reciprocal, which is the case for our applications, then $H_{xy} = H_{yx}$. As the impulse response is causal, the positive time part of (3) corresponds to the impulse response for x as a source and y as a receiver and the negative part to the time-reversed impulse response for y as a source and x as a receiver.

2.2 Guided wave tomography

Once we have obtained passive signals from passive acquisition, we can apply guided wave tomography to these data.

Here, the used guided wave tomography algorithm is based on the original iterative Hybrid Algorithm for Robust Breast Ultrasound Tomography (HARBUT) [5] but adapted to the heavy constraints imposed by the SHM framework. The principal steps are recalled here after. The first step consists in performing a time-of-flight tomography which will be the initial guess of the following diffraction tomography steps. The idea is to update iteratively the map coefficients S_{ij} with a correction $\delta_k S_{ij}^{(n)}$ based on the difference between the data $\tau_{k\to l}^{defect}$ and the computed time-of-flight $\tau_{k\to l}^{(n-1)}$ on the $(n-1)^{th}$ map:

$$\delta_k S_{ij}^{(n)} = \frac{1}{N_{ijk}}\sum_l \left(W_{ijkl}\,\frac{\tau_{k\to l}^{defect} - \tau_{k\to l}^{(n-1)}}{\lambda_{k\to l}} \right), \quad (1)$$

where $\lambda_{k\to l}$ is the trajectory's length, W_{ijkl} is a weighting of the path and N_{ijk} is a normalization factor.

Once the time-of flight tomography image is computed, it becomes the first guess of an iterative diffraction tomography process. The image is then represented thanks to an object function $O(x)$, which reads:

$$O(x) = k_0^2\left(\left(\frac{v_0}{v(x)}\right)^2 - 1\right), \quad (1)$$

where k_0 is the background wavenumber, v_0 the background phase velocity and $v(x)$ the phase velocity at position x, which is linked to the thickness thanks to the dispersion curves when the algorithm has converged. $O(x)$ can be calculated with diffraction tomography [6]. The iterative version of HARBUT consists in computing iteratively the correction $O_\delta(x)$, which is added to the previous estimation $O_b(x)$ so that $O(x) = O_b(x) + O_\delta(x)$.

3. RESULTS AND DISCUSSION

In order to test the algorithm, numerical 3D elastodynamic simulations based on the Finite Element Method (FEM) were performed. The FEM code is internally developed in the NDE department of CEA-LIST [7]. The pipe and the defect simulated are presented in figure 1.

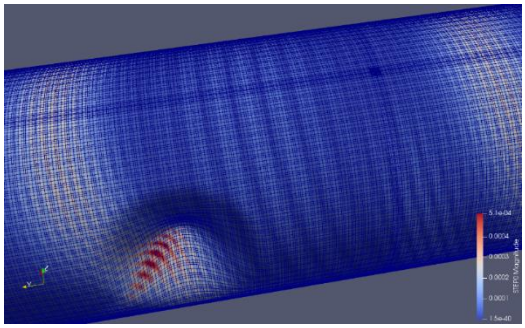

FIGURE 1: CONFIGURATION OF THE SIMULATION.

Two rings of 15 piezoelectric transducers are used to produce the signals. Then guided wave tomography algorithm is applied to this set of undersampled data. The result is presented on the figure 2. The lateral resolution is better than the axial one. This is a classic result when it comes to distributions of sensors that are not closed (limited-view imaging). This issue can be overcome with the virtual image space component iterative technique (VISCIT) [8].

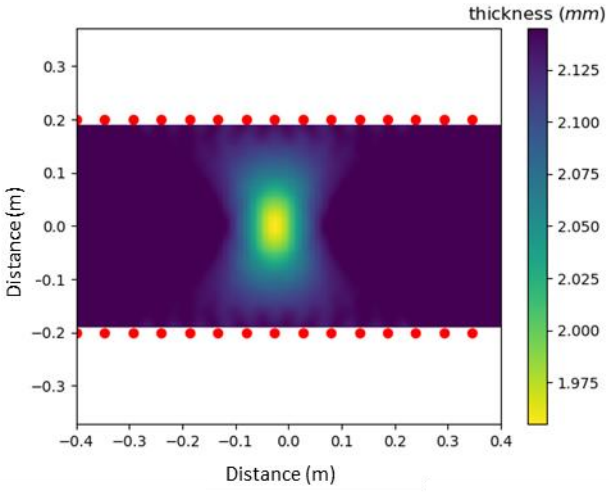

FIGURE 2: GUIDED WAVE TOMOGRAPHY WITH SIMULATED DATA.

We consider now the experimental case of a stainless steel pipe on which two rings of 15 piezoelectric transducers are glued using epoxy. The experimental setup is presented in figure 3.

First active acquisition is performed. Then, the guided wave tomography algorithm is applied to these active data. The image obtained is presented in figure 4. The defect considered is a removable magnet, which can be moved easily at different positions. It is an artificial defect that causes diffraction of guided waves, but is not representative of loss of thickness due to corrosion. That is why the image is presented in phase velocity and not in thickness.

FIGURE 3: EXPERIMENTAL SETUP.

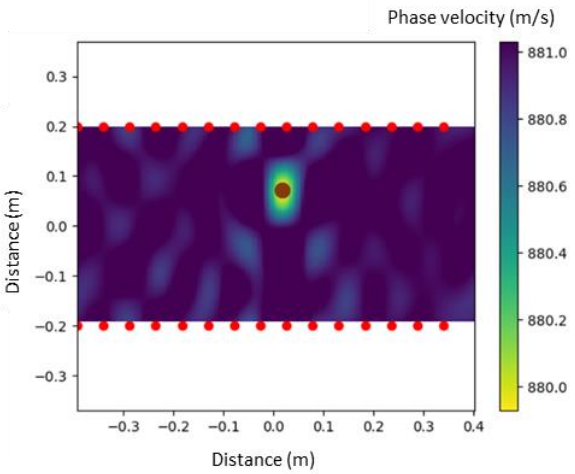

FIGURE 4: EXPERIMENTAL ACTIVE CASE

Finally, the passive acquisition case is considered. The source of noise considered here is a jet of compressed air which is applied on the intern surface of the pipe. Ten seconds of noise is acquired and then post-processed with the cross-correlation. Passive guided wave tomography is then applied to the passive signals and the result is presented in figure 5. The image obtained is slightly noisier but the position of the magnet is still well reconstructed.

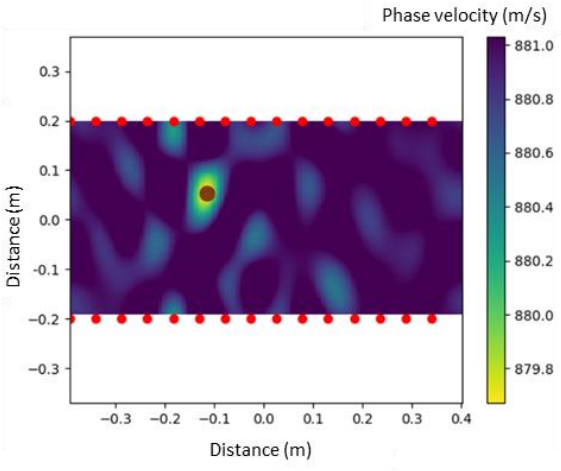

FIGURE 5: EXPERIMENTAL PASSIVE CASE

4. CONCLUSION

Passive guided wave tomography is presented in this talk. To do so, first, simulation is used in order to test the algorithm, then the active case is studied experimentally and finally passive guided wave tomography is applied in the case of a noise produced by a jet of compressed air in a pipe.

REFERENCES

[1] "SAE international, Guidelines for Implementation of Structural Health Monitoring on Fixed Wing Aircraft," 2013.

[2] T. Druet, B. Chapuis and E. Moulin, "Passive guided wave tomography for corrosion detection," in *Proceedings of the 8th EWSHM*, Bilbao, 2016.

[3] T. Druet, B. Chapuis, M. Jules, G. Laffont and E. Moulin, "Passive guided waves measurements using fiber Bragg gratings sensors," *The Journal of the Acoustical Society of America,* vol. 144, 2018.

[4] O. Lobkis and R. Weaver, "On the emergence of the Green's function in the correlations of a diffuse field," *Journal of the Acoustical Society of America,* vol. 6, pp. 3011-3017, 2001.

[5] P. Huthwaite and F. Simonetti, "High-resolution guided wave tomography," *Wave Motion,* vol. 50, pp. 979-993, 2013.

[6] P. Huthwaite, "Eliminating incident subtraction in diffraction tomography," *Proceedings of the Royal Society of London A: Mathematical, Physical and Engineering Sciences,* vol. 472, no. 2195, 2016.

[7] A. Imperiale and E. Demaldent, "A macro-element strategy based upon spectral finite elements and mortar elements for transient wave propagation modeling. Application to ultrasonic testing of laminate composite materials.," *accepted for publication in Int. J. Numer. Methods. Eng.,* 2019.

[8] P. Huthwaite, A. Zwiebel and F. Simonetti, "A new regularization technique for limited-view sound-speed imaging," *IEEE Transactions on Ultrasonics Ferroelectrics and Frequency Control,* vol. 60, no. 3, pp. 603-613, 2013.